

OPEN

Basic Hallmarks of Urothelial Cancer Unleashed in Primary Uroepithelium by Interference with the Epigenetic Master Regulator *ODC1*

Lars Erichsen¹, Hans-Helge Seifert², Wolfgang A. Schulz³, Michèle J. Hoffmann³, Günter Niegisch³, Marcos J. Araúzo-Bravo^{4,5}, Marcelo L. Bendhack⁶, Cedric Poyet⁷, Thomas Hermanns⁷, Agnes Beermann¹, Mohamed Hassan^{8,9}, Lisa Theis¹, Wardah Mahmood¹ & Simeon Santourlidis^{1*}

Urothelial carcinoma (UC) is a common disease causing significant morbidity and mortality as well as considerable costs for health systems. Extensive aberrant methylation of DNA is broadly documented in early UC, contributing to genetic instability, altered gene expression and tumor progression. However the triggers initiating aberrant methylation are unknown. Recently we discovered that several genes encoding key enzymes of methyl group and polyamine metabolism, including Ornithine Decarboxylase 1 (*ODC1*), are affected by DNA methylation in early stage UC. In this study, we investigated the hypothesis that these epigenetic alterations act in a feed-forward fashion to promote aberrant DNA methylation in UC. We demonstrate that siRNA-mediated knockdown of *ODC1* expression elicits genome-wide LINE-1 demethylation, induction of LINE-1 transcripts and double-strand DNA breaks and decreases viability in primary cultured uroepithelial cells. Similarly, following siRNA-mediated knockdown of *ODC1*, UC cells undergo double-strand DNA breaks and apoptosis. Collectively, our findings provide evidence that *ODC1* gene hypermethylation could be a starting point for the onset of genome-wide epigenetic aberrations in urothelial carcinogenesis. Furthermore, LINE-1 induction enabled by *ODC1* interference provides a new experimental model to study mechanisms and consequences of LINE-1 activation in the etiology and progression of UC as well as presumably other cancers.

Urothelial carcinoma (UC), the most common cancer of the urinary bladder, is a frequent disease with yearly 549,393 new cases and 199,922 deaths worldwide¹. Relapse rates of 30–70% and rates of progression at 10–30% for high-grade tumors present a serious health care challenge and impose enormous financial burdens on the health care systems². In particular, UC that have invaded the muscle-layers of the bladder are highly lethal.

Tobacco smoking is thought to contribute to 50% of all UC cases as a risk factor³. Aromatic amines such as 2-naphthylamin and polycyclic aromatic hydrocarbons in cigarette smoke cause mutations in key cancer-related genes by forming DNA adducts⁴. Accordingly, exposure to tobacco smoke alone is sufficient to induce

¹Epigenetics Core Laboratory, Institute of Transplantation Diagnostics and Cell Therapeutics, Medical Faculty, Heinrich-Heine University Duesseldorf, Moorenstr. 5, 40225, Duesseldorf, Germany. ²Department of Urology, University Hospital Basel, Basel, Switzerland. ³Department of Urology, Medical Faculty, Heinrich-Heine University Duesseldorf, Duesseldorf, Germany. ⁴Group of Computational Biology and Systems Biomedicine, Biodonostia Health Research Institute, 20014, San Sebastián, Spain. ⁵IKERBASQUE, Basque Foundation for Science, 48009, Bilbao, Spain. ⁶Department of Urology, University Hospital, Positivo University, Curitiba, Brazil. ⁷Department of Urology, University Hospital, University of Zurich, Zurich, Switzerland. ⁸Department of Surgery, Tulane University School of Medicine, New Orleans, LA, 70112, USA. ⁹Institut National de la Santé et de la Recherche Médicale, University of Strasbourg, 67000, Strasbourg, France. *email: simeon.santourlidis@med.uni-duesseldorf.de

transformation in urinary tract epithelial cells, which is moreover accompanied by aberrant DNA methylation⁵. Therefore urologists are advised to inform patients on the factors causing UC and strongly counsel them to stop smoking⁶.

The methylome which consists of all methylated cytosine-guanosine (CpG) dinucleotides, forms an elaborate, plastic and cell-type specific pattern in mammalian cells. It supports genome organization, gene regulation and preserves genome integrity by repressing transposable genetic elements⁷. Importantly, the methylome is influenced by exogenous factors.

Aberrant changes of the genome-wide DNA methylation pattern are broadly-documented and have long been established as an early event in the development of UC^{8–10}. Focal DNA methylation changes affect among others tumor suppressor genes¹¹ and may therefore causally contribute to the development and progression of UC. Global DNA hypomethylation, a genome-wide decrease in methylcytosine, occurs concomitantly, affecting in particular endogenous retroviruses (HERVs) and retrotransposons (SINEs and LINEs) and may result in their transcriptional reactivation¹². In particular, substantial global LINE-1 DNA hypomethylation in bladder cancer is accompanied by a shift toward expression of full-length LINE-1 elements¹³.

Expression of retrotransposons can damage the genome¹⁴. LINE-1 RNA and protein overexpression, e.g., have been linked to apoptosis, DNA damage and repair, tumor progression, cellular plasticity, and stress response¹⁴. As part of the activated LINE-1 target-primed reverse transcription (TPRT) retrotransposition mechanism, the endonuclease activity of the LINE-1 ORF2 protein generates a double-strand DNA break that recruits repair proteins to the retrotransposon insertion site. Thus, DNA damage caused by overexpression of ORF2 proteins may induce genotoxic stress and apoptosis¹⁴. It has been proposed that LINE-1 hypomethylation and activation may play a causative role in urothelial carcinogenesis by inducing genetic instability which accompanies cancer progression, especially in high-stage and high-grade cancer¹⁵. However, non-invasive and early invasive papillary transitional cell carcinomas of stages pTa and pT1, respectively, already present a plethora of genetic aberrations including losses and gains of their genetic material^{16,17}, with an increase of genomic instability when tumors progress further¹⁷.

Despite clear evidence for the involvement of an abnormal methylome and particularly LINE-1 hypomethylation in urothelial carcinogenesis it remains unknown how this process is initiated. To date, suitable *in vitro* models to investigate this issue are lacking, but are urgently required to understand both, how these epigenetic alterations are caused and how they promote cancer progression.

Recently, we have provided evidence that aberrant epigenetic regulation of key enzymes of methyl group and polyamine metabolism could be involved in establishing aberrant methylomes in UC¹⁸. Here we show for the first time that experimental downregulation of the gene encoding a key enzyme of polyamine biosynthesis, ornithine decarboxylase (*ODC1*), results in global LINE-1 hypomethylation, induction of LINE-1 transcripts, double-strand DNA breaks in primary cultured uroepithelial cells and the immortalized uroepithelial cell line HBLAK. Similarly, urothelial carcinoma cells undergo apoptosis after having acquired double-strand DNA breaks following *ODC1* interference by siRNA.

Results

***ODC1* RNA interference rapidly induces LINE-1 hypomethylation and LINE-1 transcripts in primary cultures of uroepithelial cells.** Recently, during a genome-wide screening of pTa and pT1 urothelial cancer tissue samples for altered DNA methylation, we observed distinct hypermethylation at the promoters of key genes of methyl group and polyamine metabolism pathways¹⁸. Disturbances of these key enzymes are known to lead to grave imbalances in the delicate intracellular SAM:SAH ratio resulting in genome wide DNA methylation alterations, including genome-wide LINE-1 hypomethylation^{19–21}. Therefore, we hypothesized that our observation may provide an explanation for the mechanisms involved in hypomethylation of LINE-1 retrotransposons, a hallmark of early urothelial cancer.

First, we analyzed the LINE-1 methylation status of 8 pTa and 6 pT1 early urothelial cancer tissue specimens in which we had previously observed *ODC1* promoter hypermethylation¹⁸, using idiolocal normalized real-time Methylation Specific PCR (IDLN-MSP)²². This improved method allows for a reliable comparison of LINE-1 methylation in normal and tumor tissue specimens, despite genetic heterogeneity and copy number alterations present in early urothelial cancer^{16,17}. We observed LINE-1 hypomethylation in 6 pTa and 6 pT1 urothelial carcinoma samples compared to 3 samples of healthy urothelium and 4 samples of tumor-adjacent uroepithelial tissue. Two pTa low grade tumor samples showed no hypomethylation (Fig. 1).

Next, we down-regulated *ODC1* gene expression by RNAi in the immortalized uroepithelial cell line HBLAK. This cell line developed spontaneously from a primary culture of uroepithelial cells and has a stable karyotype with few chromosomal changes²³. In addition, we applied this approach to primary, short-term cultured uroepithelial cell cultures, in order to exclude genetic and epigenetic alterations accumulating during prolonged cell cultivation as confounding factors. In both cell models, we achieved a clear repression of *ODC1* mRNA after 24 h of *ODC1* targeting by RNAi to <20% in HBLAK and <40% in primary uroepithelial cells (Fig. 2, suppl. Figure 1). *ODC1* is tightly regulated at the protein level by multiple mechanisms which control its very rapid turnover²⁴, implying that its transcriptional downregulation would lead to diminished enzyme activity within the cell. In addition, in both systems we detected a decrease in LINE-1 methylation, of 20% in HBLAK and of up to 50% in primary uroepithelial cell cultures after the first 24 h of *ODC1* downregulation. Consequently, LINE-1 transcripts increased after 48 h, with a 4-fold increase in HBLAK cells and a 2-fold increase in primary uroepithelial cell cultures. The increase in LINE-1 transcripts was paralleled by a decrease in DNA methylation of the LINE-1 promoter as demonstrated by bisulfite genomic sequencing of DNA from the same primary uroepithelial cell culture. DNA methylation in the *ODC1* RNAi-treated cells was 35.8% compared to 63.5% in non-targeting RNAi-treated cells (Fig. 3). Thus, repression of *ODC1* by RNAi rapidly results in LINE-1 hypomethylation and an increase of LINE-1 transcripts.

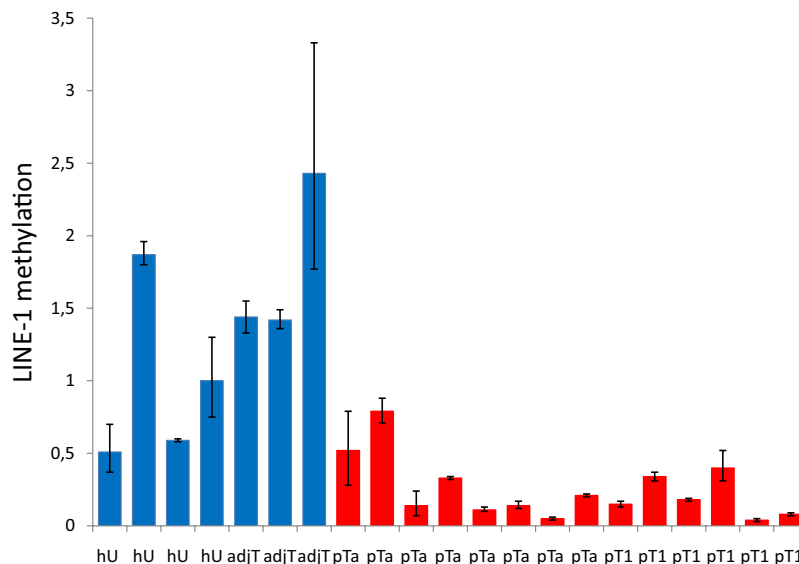


Figure 1. Relative quantification of LINE-1 methylation in early UC tissue specimens. LINE-1 methylation was measured by real time IDLN-MSPCR in four healthy-(hU), in three tumor adjacent uroepithelial (adjT), in eight pTa and in six pT1 UC tissue specimens.

***ODC1* RNA interference inhibits cell growth and induces p21 transcripts in uroepithelial cells as well as in UC cells.**

Deregulated expression of retrotransposons can damage the genome. In particular, the endonuclease activity of the LINE-1 ORF2 protein is able to generate double-strand DNA breaks, which can ultimately lead to apoptosis¹⁴, thus decreasing the number of viable cells.

Therefore we investigated cell numbers after *ODC1* RNA interference. We observed that after 24 h of RNAi treatment, uroepithelial cells undergo a substantial inhibition of cell growth (Fig. 4A). Interestingly, the same effect was observed as well in urothelial carcinoma cells (HT1376) (Fig. 4A). Expression of the cell cycle inhibitor p21 (WAF1/CIP1; *CDKN1A*) is induced by DNA damage²⁵ leading to its binding and inhibition of cyclin dependent kinases CDK1 and CDK2 and inhibition of cell cycle progression²⁶. This delay in the cell cycle enables the repair of damaged DNA. Concomitantly p21 exerts anti-apoptotic activities²⁵, prominently by binding to and inhibiting caspase 3, a crucial executor of genotoxic stress-induced apoptosis²⁷. Therefore, p21-deficient cells are more prone to undergo apoptosis after DNA damage²⁵. Interestingly, data from TCGA suggest that p21 is significantly frequently mutated in bladder cancer²⁵, a. o., the HT1376 UC cell line used here does not express p21 protein due to a frame shift mutation²⁸.

Knockdown of *ODC1* by RNA interference diminished the number of cells in a uroepithelial cell culture by approximately 50% after 24 h. This effect persisted after 48 and 72 h of RNAi treatment (Fig. 4A). The decrease in cell numbers was accompanied by a 2-fold increase of p21 transcripts at all time points in siRNA-treated cells compared to control siRNA-treated cells, in which p21 mRNA notably increased over time (Fig. 4B).

In HT1376 UC cells a 4-fold increase occurs after 48 h of treatment that extended to an 8-fold increase after 72 h (Fig. 4B).

***ODC1* RNA interference results in DNA double-strand breaks in uroepithelial cells and urothelial cancer cells and in apoptosis in urothelial cancer cells.**

To investigate whether DNA damage and apoptosis may underlie the observed decrease in cellular viability following *ODC1* downregulation, we assayed γ H2AX, an established biomarker of DNA damage response at DNA double-strand breaks²⁹. Consistently, we detected an increase of γ H2AX in *ODC1* RNAi-treated uroepithelial cells after 72 h. Similar changes were observed in HT1376 urothelial cancer cells. Higher γ H2AX levels were also detected in the supernatant of siRNA-treated cells compared to the controls (Fig. 5A). This is explained by loss of cell membrane integrity in apoptosis resulting in the release of the cellular contents, including chromatin into the environment^{30,31}.

Finally, we investigated whether cell death indeed occurred by apoptosis by assaying the active form of caspase 3/7³⁰. After 72 h of *ODC1* RNAi treatment we detected more activated caspase 3/7 activity in the treated cancer cells than in the untreated HT1376 cells (Fig. 5B).

Discussion

There is strong evidence that chemical carcinogens are involved in bladder carcinogenesis and induce mutations. However, it remains unclear which genes are affected first and constitute the crucial hits initiating the various subtypes of the disease. It is moreover unknown whether epigenetic alterations precede, accompany or follow genetic changes. Elucidating the first steps in bladder carcinogenesis could facilitate prevention and early diagnosis, and thereby lead to an improved prognosis and lower mortality rates. Previously, we showed that *ODC1* gene repression by promoter DNA methylation may be one of the first epigenetic hits in urothelial carcinogenesis (PrimeEpiHit (PEH) hypothesis)¹⁸.

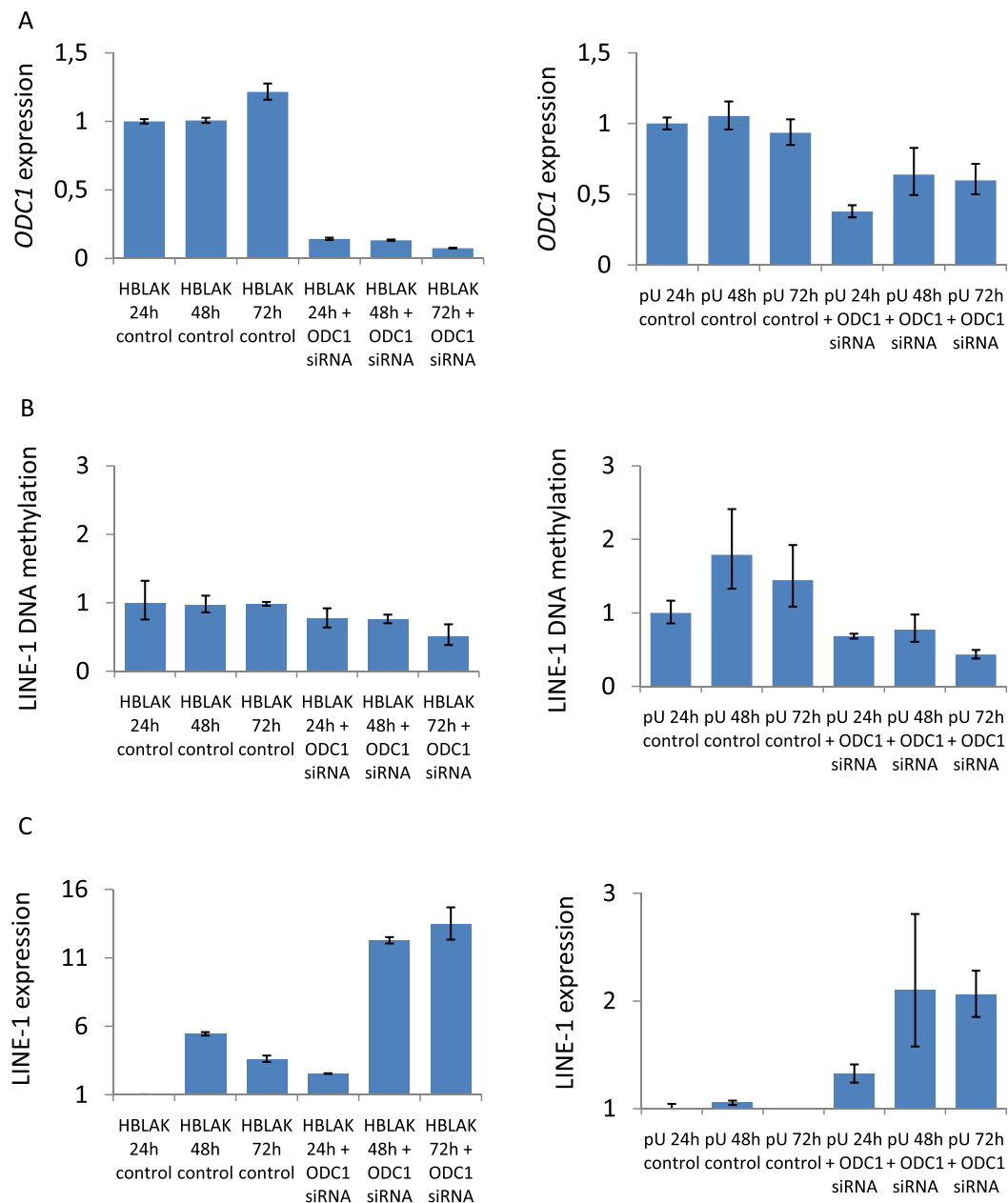


Figure 2. *ODC1* RNA interference in uroepithelial cells. *ODC1* gene expression (A), LINE-1 methylation (B), LINE-1 expression (C) in HBLAK, an immortalized uroepithelial cell line (graphs on the left) and in short-term cultured primary uroepithelial cells (graphs on the right) after downregulation of *ODC1* by RNAi over the indicated times.

ODC1 is the rate-limiting enzyme of polyamine biosynthesis and is expressed in virtually all tissues. It catalyzes the decarboxylation of ornithine to putrescine which subsequently is converted to the polyamines spermidine and spermine, by addition of propylamine groups from decarboxylated S-adenosylmethionine (dcSAM). Spermidine and spermin bind to and stabilize nucleic acids and nucleoprotein structures in the cell. In particular, they stabilize DNA and exert protection against cellular stress, for example, induced by DNA damaging agents³². Increased polyamine biosynthesis in cancer is considered important for tumor growth and survival due to increased metabolic needs³³ and constitutes a critical factor in determining sensitivity to folate depletion³⁴. Activation of *ODC1* and consequently increased concentrations of polyamines are related to tumor promotion and progression in many cancer entities. For instance *ODC1* overexpression has been reported for breast cancer, lung cancer, colon cancer, prostate cancer, pancreatic cancer, gliomas and others³³. Difluoromethylornithine (DFMO), a potent irreversible inhibitor of *ODC*, exerts cytostatic activity by diminishing levels of folate-dependent metabolites, including S-adenosylmethionine (SAM) and thymidine pools in intestinal tumors and human colorectal cancer cells³⁵ (compare suppl. Figure 2). Antitumor activity of DFMO has been supported by clinical trials on gliomas, nonmelanoma skin cancer, colon cancer and neuroblastoma³³. Noteworthy, normal intestinal epithelial cells

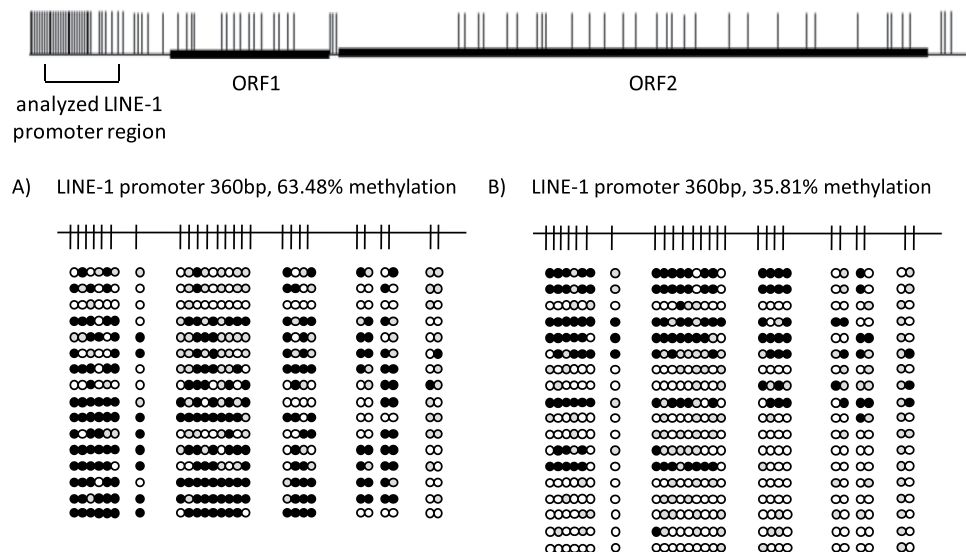


Figure 3. Bisulfite genomic sequencing of the LINE-1 promoter region in primary uroepithelial cells before and after *ODC1* RNA interference. Detailed analyses of LINE-1 promoter CpG methylation status of primary uroepithelial cells (A) and of the same uroepithelial cells after 72 h of treatment with *ODC1* RNAi (B). Black, white and grey circles stand for methylated, unmethylated and undefined CpG dinucleotides, respectively. The graph at the top of the figure depicts a schematic representation of a full-length LINE-1 retroelement with the proportional distribution of all CpG dinucleotides (short vertical strokes) and the open reading frames 1 and 2 (ORF1/2). The CpG rich region analyzed by bisulfite genomic sequencing is highlighted by a square bracket.

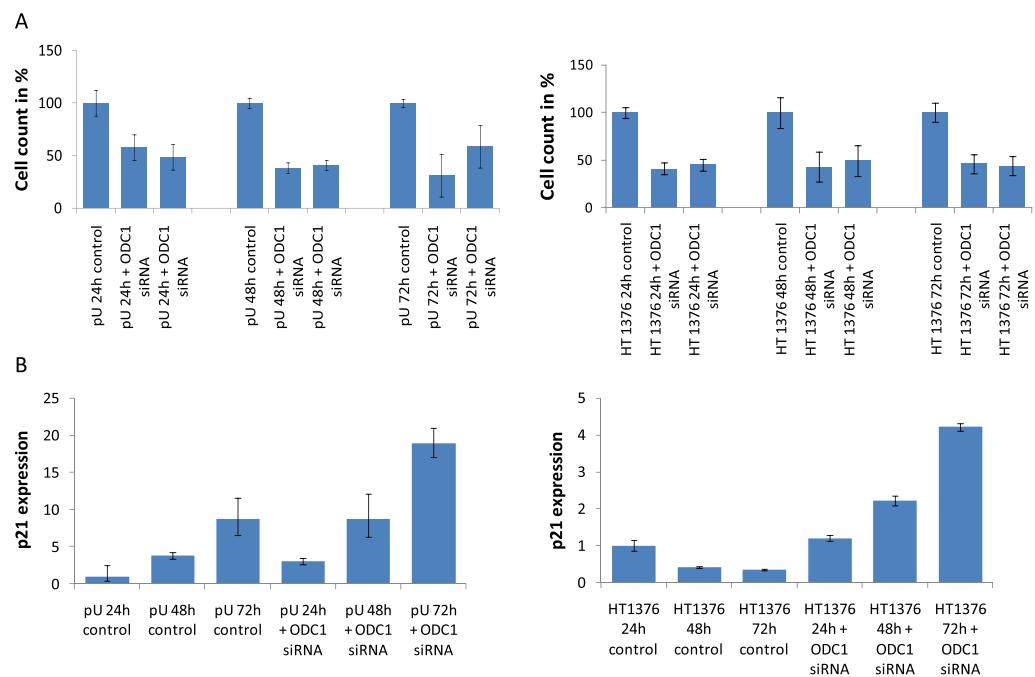


Figure 4. Cell growth and relative p21 expression in *ODC1* RNAi treated uroepithelial cells and urothelial cancer cells. Cell numbers (A) and relative p21 expression (B) were measured after treatment of cultured uroepithelial cells (graphs on the left) and HT1376 UC cells (graphs on the right) by *ODC1* RNAi for 24, 48 and 72 h, as depicted.

arrest in response to DFMO at the G1 phase of the cell cycle likely due to upregulation of p21³⁶. Likewise, human melanoma cells develop a senescence-like phenotype following DFMO treatment³⁷.

ODC1 is upregulated in many cancer types, as evidenced e.g. in the comprehensive pan-cancer “The Cancer Genome Atlas” TCGA expression data (suppl. Figure 3). However, *ODC1* mRNA expression in bladder cancer is lower than in normal bladder tissues and among the lowest of any cancer type³⁸ (suppl. Figure 3). In accord with

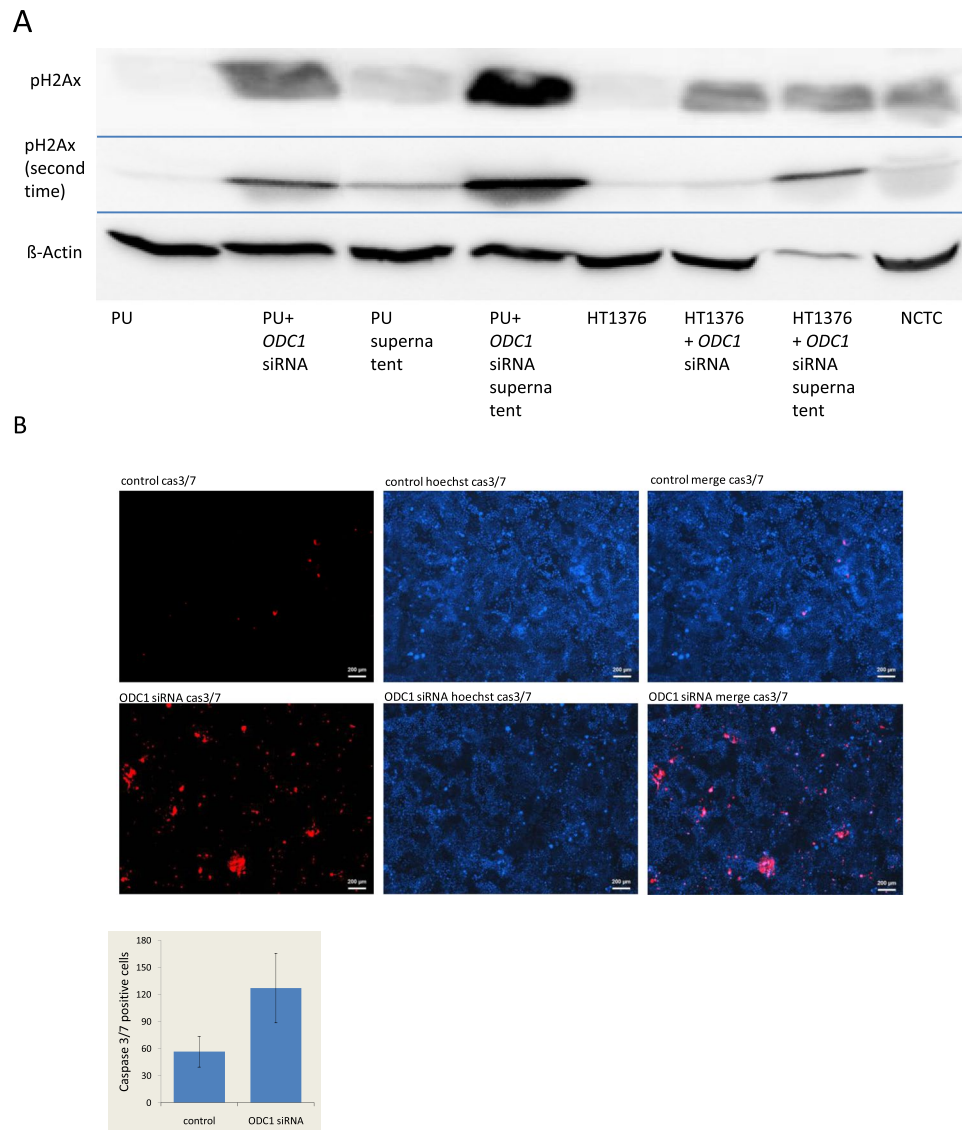


Figure 5. Detection of γ H2Ax in uroepithelial and urothelial cancer cells (UC) and Caspase 3/7 activity in UC after 72 h of *ODC1* downregulation by RNAi. γ H2Ax was determined by Western Blot analysis in uroepithelial cells, urothelial cancer cells and their cell-free culture medium supernatants before and after treatment with *ODC1* RNAi for 72 h (A) (two analyses shown). Caspase 3/7 activity was determined in HT1376 after the same treatment (B).

these findings, in an investigation of patients with various genitourinary cancers, spermidine (20%) and spermine (20%) were diminished especially in the urine of bladder patients compared to probands without bladder cancer³⁹.

DNA methylation is established as a mechanism regulating *ODC1* gene expression. In early studies a positive correlation between *ODC1* gene hypomethylation and expression was reported⁴⁰ and experimental methylation of the *ODC1* gene abolished its expression⁴¹. Furthermore aberrant *ODC1* methylation has been reported in malignant cells⁴². Recently, we demonstrated that the 5'-regulatory region of *ODC1* is hypermethylated in most analyzed early UC (pTa/pT1) specimens and that its promoter activity can be efficiently repressed by DNA methylation¹⁸. Thus we concluded that dense DNA methylation, epigenetically impairs *ODC1* expression. *ODC1* is tightly linked to methyl group metabolism since interference with its enzymatic activity results in accumulation of SAH and decarboxylated S-adenosylmethionine (dcSAM), potent competitive inhibitors of methylation reactions that cause genome-wide DNA demethylation, as shown e.g. in human oral cancer cells²⁰. Thus, hypermethylation of *ODC1* impairing *ODC1* gene expression in early urothelial cancer could act in a feed-forward fashion to promote further changes in methylation patterns, global DNA and LINE-1 hypomethylation. LINE-1 hypomethylation and activation which are established as widespread and early events in urothelial carcinogenesis would be facilitated by *ODC1* repression. LINE-1 expression in turn is thought to contribute to genetic instability during tumor progression. Mimicking *ODC1* gene repression in early stage UC and in uroepithelial cells by RNA interference *in vitro* indeed induced a comparable process as it elicited LINE-1 demethylation, LINE-1 transcriptional

Primer Name	Sequence	Product Length (bp)	Tm (°C)
sLI1met	5'-GCGCGAGTCGAAGTAGGGC-3'	193	61
asLI1met	5'-CTCCGACCAAAATATAAAATATAATCTCG-3'		
sLI1control	5'-AGGTTTTATTTTTGGGGGTAGGGTATA-3'	207	58
asLI1control	5'-CCCCTACTAAAAATACCTCCCAATTAAC-3'		

Table 1. Primers for IDLN-MSP.

activation and DNA double-strand breaks. This resulted in increased p21 expression and proliferation inhibition indicating the activation of cellular checkpoints. Consequently, diminished proliferation was observed in normal uroepithelial cells, whereas UC cells underwent apoptosis following interference with ODC1. This suggests that normal urothelial cells can respond to imbalances in methyl-group and polyamine metabolism as well as DNA damage by appropriate mechanisms, e.g. checkpoint activation, which UC cells lack. Nevertheless, if ODC1 deficiency is a frequent phenomenon in urothelial carcinogenesis, later on in the course of tumor progression, tumor cells need to adapt to it, counter or overcome it by still unknown mechanisms, which may include the impediment of checkpoints characteristic of advanced bladder cancers. Obviously, this difference in response to ODC1 repression or inhibition may provide a therapeutic window, which deserves further exploration.

Interference with ODC1, a key gene of polyamine metabolism, results in global demethylation and genetic instability. Further, we see that this may be responsible for the induction of the carcinogenesis process. With this model in hand, future research will be able to address whether this apparently crucial interference with polyamine group metabolism contributes to tumorigenesis. In addition, we will perform SAM/SAH ratio quantification of urinary S-adenosylmethionine and S-adenosylhomocysteine by stable-isotope-dilution liquid chromatography-mass spectrometry⁴³ from UC patients and healthy probands to estimate its value for early detection of UC. In addition, using the same model we will explore the role of other methyl group metabolism genes that we found concomitantly hypermethylated with *ODC1* in urothelial carcinoma, like *AHCY* and *AHCYL2*¹⁸. We therefore hypothesize that further genes of methyl group metabolism in addition to ODC1 contribute to disturbances of the methylome and thereby promote tumor progression. We are very eager to see whether the genetic integrity of these key genes mirrors DNA adduction caused by chemical carcinogens. The disruption of the genetic integrity of a gene can lead to promoter methylation and constitutive epigenetic gene silencing.

One additional aim is to develop a reliable non-invasive urinary UC diagnosis based on a combination of methylation biomarkers, e.g. LINE-1 hypomethylation and/or hypermethylated key genes, e.g. *ODC1*, *AHCY*, providing an early non-invasive detection method for the disease with high sensitivity and specificity.

Finally, LINE-1 hypomethylation and activation is a common phenomenon in many different cancers^{12,44}. To our knowledge until now there was no approach available to deliberately induce this important epigenetic alteration in normal epithelial cells. Models analogous to ours may therefore yield insights in the relationship between epigenetic alterations and carcinogenesis in other cancer types as well. Our results highlight the question to which extent, presumably temporary, disturbances in methyl-group metabolism and polyamine biosynthesis contribute to LINE-1 hypomethylation in other cancers^{12,44}. If so, the *ODC1* RNAi approach we describe here may be suitable to study the functional consequences of LINE-1 hypomethylation and its role in the carcinogenesis process of many other cancer entities as well.

Methods

Tissue samples. *Cell lines and cell cultures.* Cultivation of primary uroepithelial cells and HBLAK cells was performed as described by Swiatkowski *et al.* and Hoffmann *et al.*^{45,46}. The UC cell line HT1376 was isolated from a high grade urothelial cancer of a 58 years old female patient⁴⁷ and was kindly provided by the DSMZ (Braunschweig, Germany).

Preparation of DNA from formalin-fixed, paraffin-embedded (FFPE) tissue samples. All methods were carried out in accordance with relevant guidelines and regulations. We confirm that the experimental protocols were approved and informed consent was obtained from all participants. An appropriate ethics vote was granted by the Kantonale Ethikkommission Zürich on 22.02.2013, Ref. Nr. KEK-ZH-Nr 2012–0352. All samples were prepared as previously described in detail¹⁸.

The tissue samples were pathologically reviewed, microdissected and prepared as previously described¹⁸. In Fig. 1, from left to right, all pTa samples but sample number 4 (high grade) are low grade and all pT1 samples but sample number 1 (low grade) are high grade UC samples.

Relative Quantification of LINE-1 methylation in UC and reference samples by real-time MSP. Real time Methylation-Specific PCR of differentially methylated LINE-1 promoter regions was performed as follows: Bisulfite-converted DNA of the tissue samples served as template for amplification of methylated LINE-1 sequences in a normalized real time MSP approach for genetic imbalanced DNA specimens as described²². The primers used are listed in Table 1. The amplification conditions were denaturation at 95 °C for 10 min, followed by 40 cycles of 95 °C for 30 s, Tm for 40 s and 72 °C for 15 s.

ODC1 RNA interference. 400.000 (primary urothelium) or 50.000 (HT1376) cells per well were seeded in 6-well plates (Sarstedt, Nümbrecht, Germany). 40 pmol of siRNA (2 µl) (Human ODC1 (4953) siRNA, M-006668-00-0005 - SMARTpool or siGENOME Non-Targeting siRNA Pool, D-001206-14-05, Dharmacon) were mixed

Primer Name	Sequence	Product Length	TM
sLINEkonv1AmpI	5'-GGTTTATTTTATTAGGGAGTGTAG-3'	436	51
asLINEkonv1AmpI	5'-ACAAAAACAAACAACTCC-3'		

Table 2. Primers for LINE-1 bisulfite genomic sequencing.

Primer Name	Sequence	Product Length (bp)	TM (°C)
s1GAPDHmrna	5'-CATGACAACCTTGGTATCGTGGA-3'	381	62
as1GAPDHmrna	5'-GTGGGTGTCGCTGTTGAAGTC-3'		
s1ODC1mrna	5'-CCGCTCGAGCGGATAAGTAGGGAGCGCGCTG-3'	276	54
as1ODC1mrna	5'-ATCATGGCGACCTACTCTTAC-3'		
s1LINEmRNA	5'-TGGAATAGGTGTGGTGTGGTGTCT-3'	246	61
as1LINEmRNA	5'-TCACTCAGGACAGCCAGACG-3'		
sp21mrna	5'-GGAAGACCATGTGGACCTGT-3'	146	55
asp21mrna	5'-GGCGTTTGGAGTGGTAGAAA-3'		

Table 3. Primers for real-time PCR.

with 248 μ l Opti-MEM (1 \times) medium (Gibco). 5 μ l of Lipofectamine 2000 (Dharmacon) were mixed with 245 μ l Opti-MEM (1 \times) medium (Gibco). All mixes were incubated for 5 mins at RT. Then every siRNA mix was mixed together with the Lipofectamine mix and incubated for additional 20 mins at RT. Afterwards, 500 μ l of the final mix was added to each well. Cells were kept in the incubator at 37 °C for 24 h, 95% humidity and 5% CO₂. Retransfection with siRNA was performed every 24 h for three times.

Bisulfite genomic sequencing. Bisulfite sequencing was performed following bisulfite conversion with the EpiTect Kit (Qiagen, Hilden, Germany) as described^{48–50}. PCR primers for specific amplification of LINE-1 promoter sequences are listed in Table 2. The amplification conditions were denaturation at 95 °C for 13 min, followed by 35 cycles of 95 °C for 50 s, 51 °C for 45 s, and 72 °C for 30 s. We used 10–20 ng of bisulfite converted DNA, x μ l of a 200 μ M dNTP Mix solution (Promega), 10 pm of each primer and 1.5 units of HotStarTaq DNA Polymerase (Qiagen) per reaction. The amplification product was 436 bp. The TA Cloning Kit (Invitrogen) was used for cloning of the amplification products according to the manufacturer's instructions. Sequence evaluation was performed with the BigDye Terminator Cycle Sequencing Kit (Applied Biosystems) on a DNA analyzer 3700 (Applied Biosystems) using the M13-as primer. On average 30 clones were sequenced to obtain the methylation profile of one sample. All sequences were aligned using CLUSTLW from the Kyoto University Bioinformatics Center on <http://www.genome.jp/tools/clustalw/> and all methylated CpGs were manually counted for every single CpG position.

RNA preparation, cDNA synthesis, and real-time PCR. RNA was prepared using the RNeasy Mini Kit (Qiagen) according to the manufacturer's instructions. First-strand cDNA synthesis was performed from 1.5 μ g RNA by reverse transcription using oligo(dT) (Promega) and Moloney murine leukemia virus reverse transcriptase (Promega) in a volume of 50 μ l at 42 °C for 1 h. Real-time PCR was carried out with SYBR Green PCR Mastermix (Applied Biosystems) using 25 ng template cDNA. All reactions were run in triplicates on a StepOnePlus System (Applied Biosystems, Foster City, CA). Standard curves were generated using StepOne software v2.1 (Applied Biosystems). Relative changes in gene expression were calculated following the $\Delta\Delta$ Ct-method with glyceraldehyde-3-phosphate dehydrogenase (GAPDH) mRNA as a standard. Primers were designed after excluding pseudogenes or other closely related genomic sequences which could interfere with specific amplification by amplicon and primer sequences comparison in BLAT sequence data base (<https://genome.ucsc.edu/FAQ/FAQblat.html>) Table 3.

Determination of cell numbers. After siRNA treatment the cell numbers were determined using a Neubauer counting chamber (Bürker, Friedrichsdorf, Germany). 10 μ l of each cell suspension was mixed with 10 μ l trypan blue (0.4%) (Gibco) and pipetted into the chamber. Four large corner squares were counted under an inverse laboratory microscope (Leica). Cell numbers were calculated with the following formula: cell/ml = average of the number of cells counted over all squares \times chamber factor \times dilution factor.

Western blot. Primary uroepithelial cells and HT1376 urothelial cancer cells and NCCIT teratocarcinoma cells were lysed in lysis buffer containing 5 M NaCl, 1% NP-40, 0.5% DOC, 0.1% SDS, 1 mM EDTA, 50 mM Tris, pH 8.0, and freshly added 10 μ l/mL protease inhibitor (Sigma, Munich, Germany). 15 μ g of protein was resolved in a 12% sodium dodecyl sulfate-PAGE gel and transferred onto Immobilon-P membrane (Millipore). Membranes were probed with primary antibody against Phospho-Histone H2A.X (Ser139) (20E3, Rabbit mAb, Cell Signaling, Frankfurt, Germany) and β -Actin (8H10D10 Mouse mAb, Cell Signaling, Frankfurt, Germany) at 4 °C overnight, washed with 0.1% Tween-20 in Tris-buffered saline, and incubated with secondary antibody conjugated with horseradish peroxidase. The signals were visualized with enhanced luminescence (WesternBright Quantum, Advansta, Ort, Land).

Apoptosis detection. Apoptosis assay was performed using the ImageIT Live Red Caspase-3 and -7 Detection Kit (Thermo Fisher Scientific, Ort, Land) according to the manufacturer's instructions. In brief, cells were seeded in a 12 well plate (Sarstedt, Ort, Land). After treatment with siRNA for 72 h, the cells were washed with PBS and incubated with a 30-fold dilution of the provided FLICA reagent for 60 min at 37 °C for 24 h, 95% humidity and 5% CO₂. After this incubation the cells were washed again with PBS and nuclei were stained with HOECHST 33342 (Thermo Fisher Scientific). To remove the Hoechst solution two additional washing steps with a 1x dilution of the provided wash buffer were carried out for 5 mins at RT and cells were counted using a fluorescent microscope X-Cite Series 120 (Lumen Dynamics, Ort, Land).

Received: 12 July 2019; Accepted: 14 February 2020;

Published online: 02 March 2020

References

1. Ferlay, J. *et al.* Global Cancer Observatory: Cancer Today. Lyon, France: International Agency for Research on Cancer. Available from: <https://gco.iarc.fr/today>, accessed [22 02 2019].
2. Satek, R. S. *et al.* The economics of bladder cancer: costs and considerations of caring for this disease. *Eur. Urol.* **66**, 253–62 (2014).
3. Leal, J. Association between smoking and risk of bladder cancer among men and women. *JAMA.* **306**, 737–45 (2011).
4. Besaratinia, A. *et al.* Genotoxicity of tobacco smoke-derived aromatic amines and bladder cancer: current state of knowledge and future research directions. *FASEB J.* **27**, 2090–100 (2013).
5. Brait, M. *et al.* Genome-wide methylation profiling and the PI3K-AKT pathway analysis associated with smoking in urothelial cell carcinoma. *Cell Cycle.* **1**, 1058–70 (2013).
6. Brausi, M. A. Primary prevention and early detection of bladder cancer: two main goals for urologists. *Eur. Urol.* **63**, 242–3 (2013).
7. Bird, A. DNA methylation patterns and epigenetic memory. *Genes Dev.* **16**, 6–21 (2002).
8. Maruyama, R. *et al.* Aberrant promoter methylation profile of bladder cancer and its relationship to clinicopathological features. *Cancer Res.* **61**, 8659–63 (2001).
9. Salem, C. *et al.* Progressive increases in de novo methylation of CpG islands in bladder cancer. *Cancer Res.* **60**, 2473–6 (2000).
10. Catto, J. W. F. *et al.* Promoter hypermethylation is associated with tumor location, stage, and subsequent progression in transitional cell carcinoma. *J. Clin Oncol.* **23**, 2903–10 (2005).
11. Kandimalla, R. *et al.* DNA methylation-based biomarkers in bladder cancer. *Nat. Rev. Urol.* **10**, 327–35 (2013).
12. Schulz, W. A. Methylation of endogenous human retroelements in health and disease. *Curr. Top Microbiol.* **310**, 211–50 (2006).
13. Kreimer, U. *et al.* HER-K and LINE-1 DNA Methylation and Reexpression in Urothelial Carcinoma. *Front. Oncol.* **26**, 255 (2013).
14. Goodier, J. L. Restricting retrotransposons: a review. *Mob. DNA.* **11**, 16 (2016).
15. Florl, A. R. *et al.* DNA methylation and expression of LINE-1 and HER-K proirous sequences in urothelial and renal cell carcinomas. *Br. J. Cancer.* **80**, 1312–21 (1999).
16. Simon, R. *et al.* Chromosomal aberrations associated with invasion in papillary superficial bladder cancer. *J. Pathol.* **185**, 345–351 (1998).
17. Prat, E. *et al.* Detection of chromosomal imbalances in papillary bladder tumors by comparative genomic hybridization. *Urology.* **57**, 986–92 (2001).
18. Erichsen, L. *et al.* Aberrant methylated key genes of methyl group metabolism within the molecular etiology of urothelial carcinogenesis. *Sci. Rep.* **22**, 3477 (2018).
19. Tsuji, T. *et al.* Induction of epithelial differentiation and DNA demethylation in hamster malignant oral keratinocyte by ornithine decarboxylase antizyme. *Oncogene.* **4**, 24–33 (2001).
20. Yamamoto, D. *et al.* Ornithine decarboxylase antizyme induces hypomethylation of genome DNA and histone H3 lysine 9 dimethylation (H3K9me2) in human oral cancer cell line. *PLoS One* **3**, e12554 (2010).
21. Chen, Z. *et al.* Mice deficient in methylenetetrahydrofolate reductase exhibit hyperhomocysteinemia and decreased methylation capacity, with neuropathology and aortic lipid deposition. *Hum. Mol. Genet.* **1**, 433–43 (2001).
22. Santourlidis, S. *et al.* IDLN-MSP: Idiomatic normalization of real-time methylation-specific PCR for genetic imbalanced DNA specimens. *Biotechniques.* **60**, 84–7 (2016).
23. Hoffmann, M. J. *et al.* The New Immortalized Uroepithelial Cell Line HBLAK Contains Defined Genetic Aberrations Typical of Early Stage Urothelial Tumors. *Bladder. Cancer.* **2**, 449–463 (2016).
24. Perez-Leal, O. *et al.* Regulation of polyamine metabolism by translational control. *Amino Acids.* **42**, 611–7 (2012).
25. El-Deiry, W. S. p21(WAF1) Mediates Cell-Cycle Inhibition, Relevant to Cancer Suppression and Therapy. *Cancer Res.* **76**, 5189–91 (2016).
26. Cmieloá, J. p21Cip1/Waf1 protein and its function based on a subcellular localization. *J. Cell. Biochem.* **112**, 3502–6 (2011).
27. Choudhary, G. S. *et al.* Caspase-3 activation is a critical determinant of genotoxic stress-induced apoptosis. *Methods Mol. Biol.* **1219**, 1–9 (2015).
28. Makri, D. *et al.* WAF1/p21 regulates proliferation, but does not mediate p53-dependent apoptosis in urothelial carcinoma cell lines. *Int. J. Oncol.* **12**, 621–8 (1998).
29. Georgoulis, A. *et al.* Genome Instability and γ H2AX. *Int. J. Mol. Sci.* **18**, (9) (2017).
30. Elmore, S. Apoptosis: a review of programmed cell death. *Toxicol. Pathol.* **35**, 495–516 (2007).
31. Choi, J. J. *et al.* Release of DNA from dead and dying lymphocyte and monocyte cell lines *in vitro*. *Scand. J. Immunol.* **60**, 159–66 (2004).
32. Nayelt, I. *et al.* DNA condensation by chiral alpha-methylated polyamine analogues and protection of cellular DNA from oxidative damage. *Biomacromolecules.* **11**, 97–105 (2010).
33. Alexiou, G. A. *et al.* Difluoromethylornithine in cancer: new advances. *Future Oncol.* **13**, 809–819 (2017).
34. Bistulfi, G. *et al.* Polyamine biosynthesis impacts cellular folate requirements necessary to maintain S-adenosylmethionine and nucleotide pools. *FASEB J.* **23**, 2888–97 (2009).
35. Witherspoon, M. *et al.* Unbiased metabolite profiling indicates that a diminished thymidine pool is the underlying mechanism of colon cancer chemoprevention by alpha-difluoromethylornithine. *Cancer Disco.* **3**, 1072–81 (2013).
36. Li, L. *et al.* JunD stabilization results in inhibition of normal intestinal epithelial cell growth through p21 after polyamine depletion. *Gastroenterology.* **123**, 764–779 (2002).
37. Kramer, D. L. *et al.* Polyamine depletion in human melanoma cells leads to G1 arrest associated with induction of p21WAF1=CIP1=SDI1, changes in the expression of p21-regulated genes, and a senescence-like phenotype. *Cancer Res.* **61**, 7754–7762 (2001).
38. Robertson, A. G. *et al.* Comprehensive Molecular Characterization of Muscle-Invasive Bladder. *Cancer. Cell.* **9**, 1033 (2017).
39. Sakai, S. *et al.* Detection of urinary polyamine by a new enzymatic differential assay. (III). Studies on urinary polyamines in patients with malignant genitourinary diseases. *Hinyokika Kyo.* **32**, 343–50 (1986).
40. Jänne, J. *et al.* Molecular genetics of ornithine decarboxylase in human tumor cells. *Ad. Enzyme Regul.* **28**, 81–91 (1989).

41. Halmekytö, M. *et al.* Methylation of human ornithine decarboxylase gene before transfection abolishes its transient expression in Chinese hamster oary cells. *Biochem. Biophys Res. Commun.* **14**, 528–34 (1989).
42. Wahlfors, J. Certain changes in ornithine decarboxylase gene methylation accompany gene amplification. *Biochem J.* **15**, 435–40 (1991).
43. Stabler, S. P. *et al.* Quantification of serum and urinary S-adenosylmethionine and S-adenosylhomocysteine by stable-isotope-dilution liquid chromatography-mass spectrometry. *Clin. Chem.* **50**, 365–72 (2004).
44. Wilson, A. S. *et al.* DNA hypomethylation and human diseases. *Biochim. Biophys Acta.* **1775**, 138–62 (2007).
45. Swiatkowski, S. *et al.* Actiities of MAP-kinase pathways in normal uroepithelial cells and urothelial carcinoma cell lines. *Exp. Cell Res.* **282**, 48–57 (2003).
46. Hoffmann, M. J. *et al.* The New Immortalized Uroepithelial Cell Line HBLAK Contains Defined Genetic Aberrations Typical of Early Stage Urothelial Tumors. *Bladder Cancer.* **2**, 449–463 (2016).
47. Rasheed, S. *et al.* Human bladder carcinoma: characterization of two new tumor cell lines and search for tumor iruses. *J. Natl Cancer Inst.* **58**, 881–90 (1977).
48. Ghanjati, F. *et al.* Unresered application of epigenetic methods to define differences of DNA methylation between urinary cellular and cell-free DNA. *Cancer Biomark.* **14**, 295–302 (2014).
49. Santourlidis, S. *et al.* Crucial role of DNA methylation in determination of clonally distributed killer cell Ig-like receptor expression patterns in NK cells. *J. Immunol.* **169**, 4253–61 (2002).
50. Santourlidis, S. *et al.* Unrestricted somatic stem cells (USSC) from human umbilical cord blood display uncommitted epigenetic signatures of the major stem cell pluripotency genes. *Stem. Cell Res.* **6**, 60–9 (2011).

Acknowledgements

Simeon Santourlidis wishes to dedicate this work in Memoriam and in Gratitude to Professor Rolf Ackermann. His intense efforts and his valuable advices have decisively support and impact my work. The authors thank the Comprehensie Cancer Center, Uniernitätsklinikum Düsseldorf (Tumorbank des UTZ) for providing samples. This study was financially supported by: Prof. Dr. Rolf Ackermann, Wissenschaftliche Urologische Gesellschaft e.V., PTJ Jülich. Stiftung für Altersforschung (Foundation for Aging Research), Heinrich-Heine-Uniernität Düsseldorf. Prof. Dr. med. Hans-Helge Seifert, Uniernitätsspital Basel. Simeon Santourlidis thanks Prof. James Adjaye (Institute for Stem Cell Research and Regeneratie Medicine, Medical Faculty, Heinrich Heine Uniernity, Düsseldorf) for his important support of this study in a decisive situation. We are thankful to Johannes Fischer (Institute of Transplantation Diagnostics and Cell Therapeutics, Medical Faculty, Heinrich-Heine Uniernity Duesseldorf) for his efforts to provide additional financial support.

Author contributions

Lars Erichsen: experiments, supplementary data, data interpretation. Hans-Helge Seifert: isolation, collection of patient samples, data interpretation, establishment of cultivation of primary uroepithelium. Cedric Poyet, Thomas Hermanns: isolation, selection and collection of patient samples, data interpretation, clinical advice. Wolfgang A. Schulz: data interpretation, supply of cell lines and manuscript revision. Günter Niegisch, Michele J. Hoffmann: data interpretation, supply of cell lines and primary uroepithelium. Agnes Beermann: experiments. Lisa Theis: experiments. Wardah Mahmood: experiments. Marcelo L. Bendhack: data interpretation, clinical advice and manuscript revision. Mohamed Hassan: data interpretation and support of apoptosis experiments. Marcos-Arauzo Brao: bioinformatics, data interpretation and manuscript revision. Simeon Santourlidis: study conception and design, supervision of epigenetic methods, data interpretation, manuscript writing.

Competing interests

The authors declare no competing interests.

Additional information

Supplementary information is available for this paper at <https://doi.org/10.1038/s41598-020-60796-8>.

Correspondence and requests for materials should be addressed to S.S.

Reprints and permissions information is available at www.nature.com/reprints.

Publisher's note Springer Nature remains neutral with regard to jurisdictional claims in published maps and institutional affiliations.



Open Access This article is licensed under a Creative Commons Attribution 4.0 International License, which permits use, sharing, adaptation, distribution and reproduction in any medium or format, as long as you give appropriate credit to the original author(s) and the source, provide a link to the Creative Commons license, and indicate if changes were made. The images or other third party material in this article are included in the article's Creative Commons license, unless indicated otherwise in a credit line to the material. If material is not included in the article's Creative Commons license and your intended use is not permitted by statutory regulation or exceeds the permitted use, you will need to obtain permission directly from the copyright holder. To view a copy of this license, visit <http://creativecommons.org/licenses/by/4.0/>.

© The Author(s) 2020